Cell Reports, Volume *22*

Supplemental Information

Innate Immune Signaling in *Drosophila* Blocks Insulin Signaling by Uncoupling $PI(3,4,5)P_3$ Production and Akt Activation

Stephen W. Roth, Moshe D. Bitterman, Morris J. Birnbaum, and Michelle L. Bland

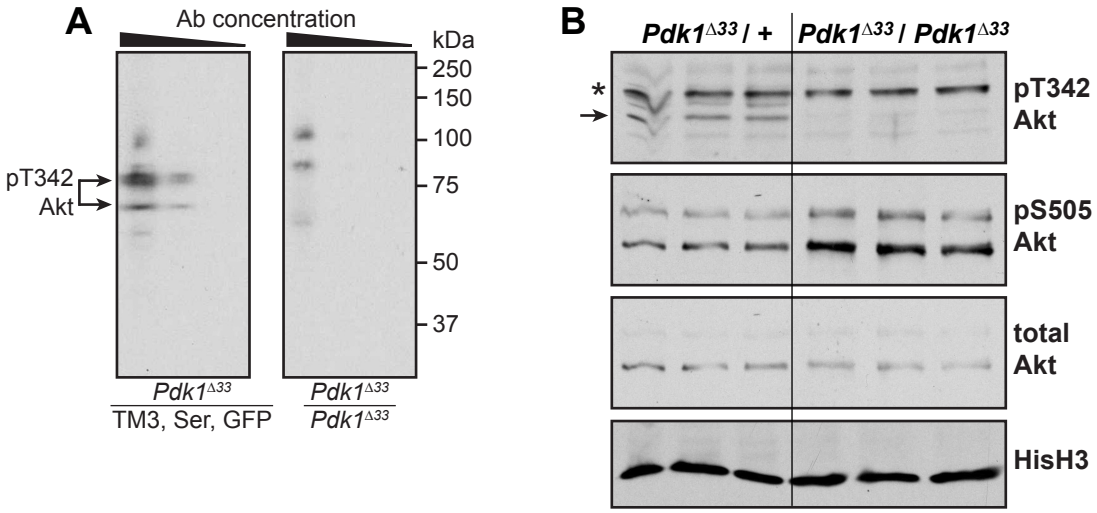

Figure S1. Validation of a novel rabbit anti-phosphoThr342-Akt antibody, Related to Figures 1 and 3. **A)** A rabbit anti-phosphoThr342-Akt antibody was raised against a phosphorylated peptide and affinity purified. Serial dilutions of anti-sera were tested against lysates from larvae heterozygous (left) or homoozygous (right) for the strong, hypomorphic *Pdk1*$^{\Delta 33}$ mutation. The antibody detects signal in *Pdk1*$^{\Delta 33}$ heterozygotes but not homozygotes at ~66 and 85 kDa (arrows), consistent with the reported molecular weights of Akt splice variants (Andjelkovic et al., 1995). **B)** Western blot analysis of phosphorylated (pT342 and pS505) and total Akt and Histone H3 (HisH3) in larvae heterozygous (left, n = 2 animals/lane) or homozygous (right, n = 10 animals/lane) for *Pdk1*$^{\Delta 33}$. The arrow points to phospho-T342 Akt, the higher molecular weight band (*) is non-specific.

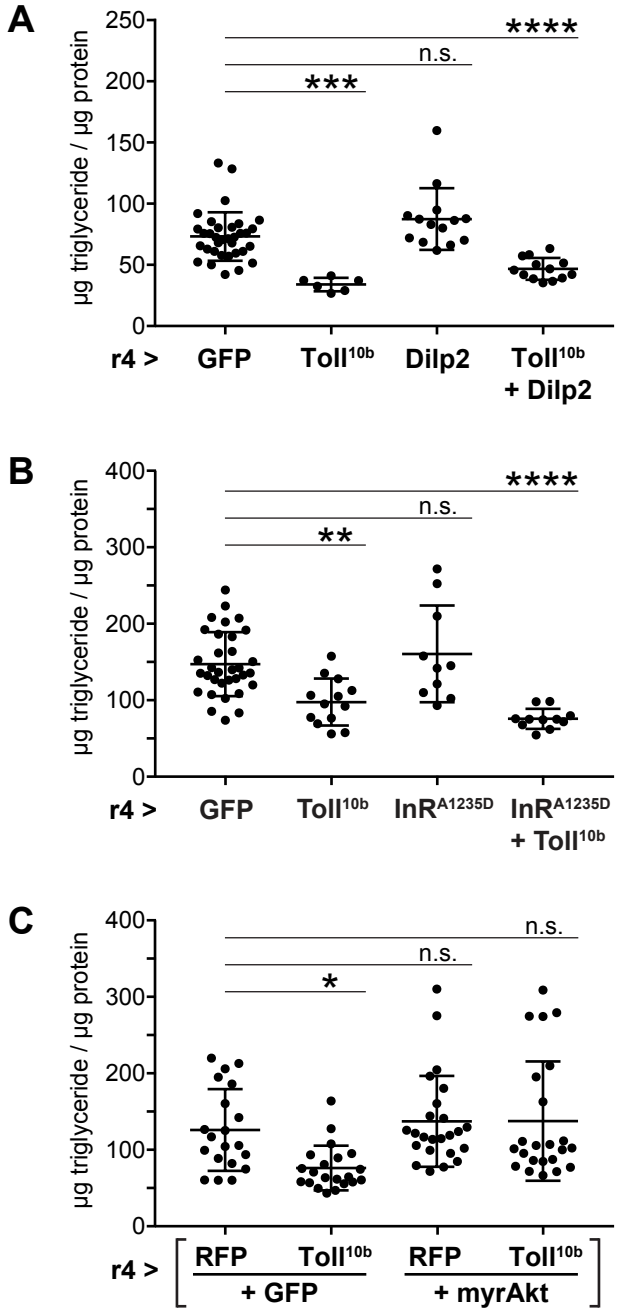

Figure S2. Toll signaling acts downstream of the insulin receptor and upstream of Akt to suppress triglyceride storage, Related to Figure 1.

Triglyceride levels were measured and normalized to protein in whole animal lysates of mid-third instar larvae expressing the following transgenes in fat body under control of r4-GAL4: **A)** GFP, Toll^{10b}, Dilp2, or Toll^{10b} + Dilp2, n = 6-14/gp, except GFP, n = 34, ****p < 0.0001 and ***p = 0.0002 versus GFP; **B)** GFP, Toll^{10b}, InR^{A1325}, or InR^{A1325} + Toll^{10b}, n = 10-13/gp, except GFP, n = 33, **p = 0.0013 and ****p < 0.0001 versus GFP; **C)** RFP + GFP, Toll^{10b} + GFP, RFP + myrAkt, or Toll^{10b} + myrAkt, n = 20-23/gp, *p = 0.0207 versus RFP+GFP. Data are presented as mean ± S.D.

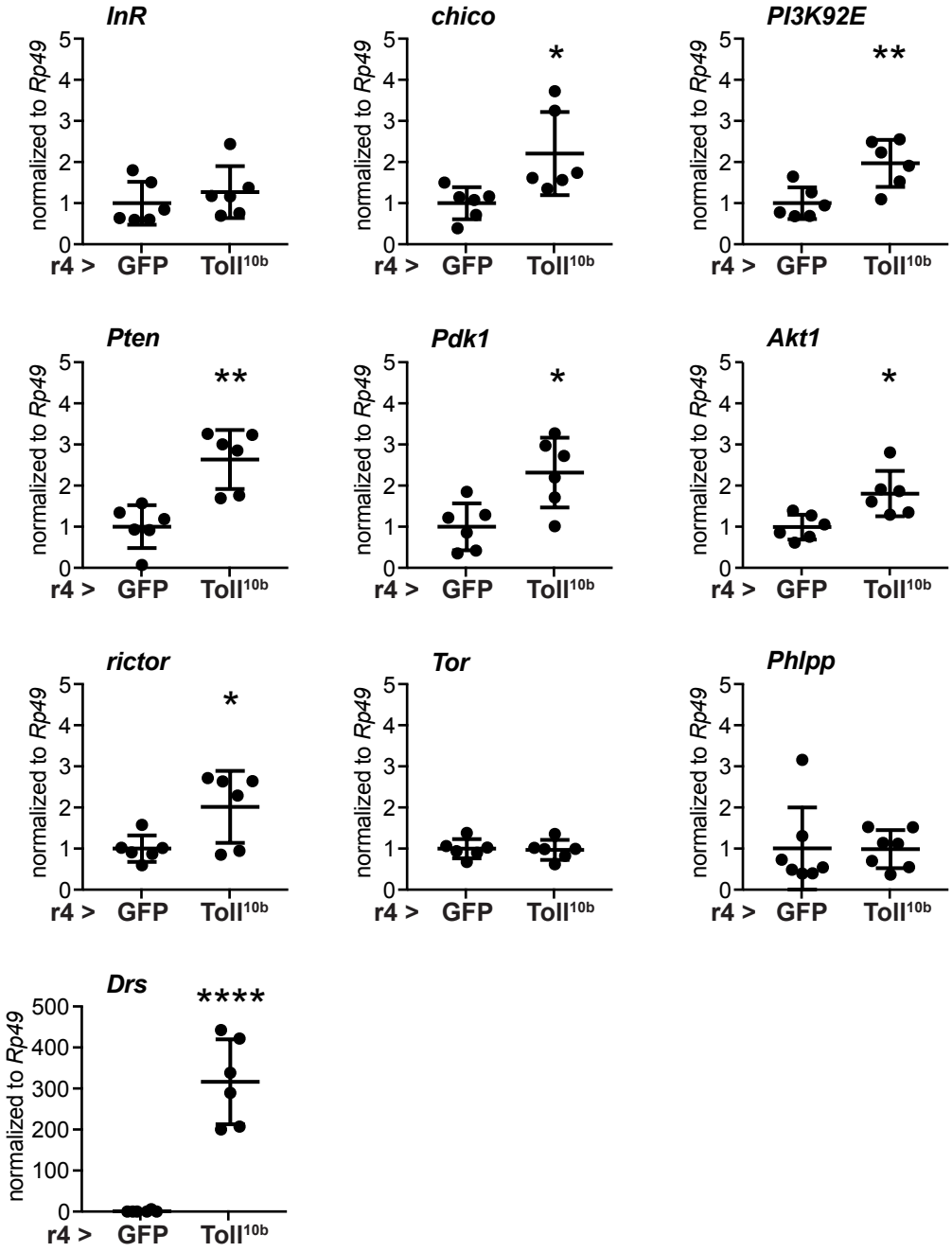

Figure S3. Insulin signaling pathway gene expression in fat bodies with active Toll signaling, Related to Figure 3.

RNA was isolated from mid-third instar larval fat bodies expressing GFP or Toll^{10b} under control of r4-GAL4. Transcript levels of *InR*, *chico*, *PI3K92E* (encodes Dp110), *Pten*, *Pdk1*, *Akt1*, *rictor*, *Tor*, *Phlpp* and *Drs* were measured in equal amounts of cDNA by Q-PCR. All transcripts are normalized to *Rp49* levels, which did not differ between genotypes. *Drs* encodes Drosomycin, a canonical antimicrobial peptide target gene of the Toll signaling pathway. *$p < 0.05$, **$p < 0.01$ and ****$p < 0.0001$ versus GFP, n = 6-7 samples/genotype. Data are presented as mean ± S.D.

A ***Pdk1*, 3' exons**

B **Wild type allele**

GCTATGCTATCCACTGGTCGGAAGCTATTGAGAACATGCGCAAGTTGGCCTACGGAGATCCCTCCTCCACATCTGCAGT
GTCCTGCTCCAGCGGCAGCAGTAATAGCCTGGCTGTCATCTCAAATTCATCCGCCGCCTCCTCAAGCAATTCGCCCACG
GTGAAACGCAGTTCCCCCGTAAACGCTCCTCAAGCTTCGACGGCGTCTGACAACCGGACATTGGGTAGCACCAGAACGG
G**GACGTCACCTAGCAAGAAGACGG**CGTCTAAG**TAA**ACGTAGTCCTATTTATAGCAATGTGAAATTAATTTAGTTGAAAT
TTAGTGCAAACGAAGCGATGGCGTAGAAGAGGGCGGGAATAGAAGTAAGCTTAGAAGTAGAAGTAAGTGATGAAGGGGA
AATAATGATCGTGTCTCTAGTGCTAATTAGAACCAAATTTCTGTTTTCCGATTTGTATTGTGCTTAGGGCG

ssDNA template for homology-directed repair

AGCTTCGACGGCGTCTGACAACCGGACATTGGGTAGCACCAGAACGGG**GACGTCACCTAGCAAGAAGAC*AA***CGTCTAAG
ATGGAGCAGAAGCTGATCTCCGAGGAGGATCTGTAAATAACGTAGTCCTATTTATAGCAATGTGAAATTAATTTAGTTG
AAATTTAGTGCAAACGAAGCGATGGCGTAGAAGAGGGCGGGA

Modified allele

GCTATGCTATCCACTGGTCGGAAGCTATTGAGAACATGCGCAAGTTGGCCTACGGAGATCCCTCCTCCACATCTGCAGT F1
GTCCTGCTCCAGCGGCAGCAGTAATAGCCTGGCTGTCATCTCAAATTCATCCGCCGCCTCCTCAAGCAATTCGCCCACG
GTGAAACGCAGTTCCCCCGTAAACGCTCCTCAAGCTTCGACGGCGTCTGACAACCGGACATTGGGTAGCACCAGAACGG
G**GACGTCACCTAGCAAGAAGAC*AA***CGTCTAAG**ATGGAGC**AGAAGCTGATCTCCGAGGAG**GATCTG**TAA**ATAACG**TAG**TC R2
CTATTTATAGCAATGTGAAATTAATTTAGTTGAAATTTAGTGCAAACGAAGCGATGGCGTAGAAGAGGGCGGGAATAGA
AGTAAGCTTAGAAGTAGAAGTAAGTGATGAAGGGGAAATAATGATCGTGTCTCTAGTGCTAATTAGAACCAAATTTCTG
TTTTCCGATTTGTATTGTGCTTAGGGCG R1

C

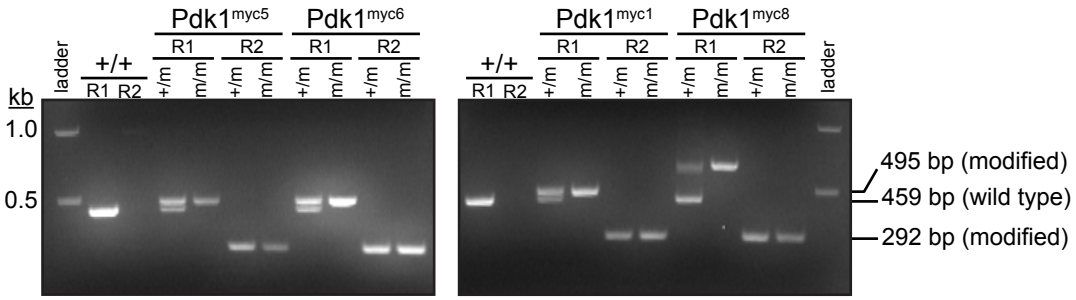

D

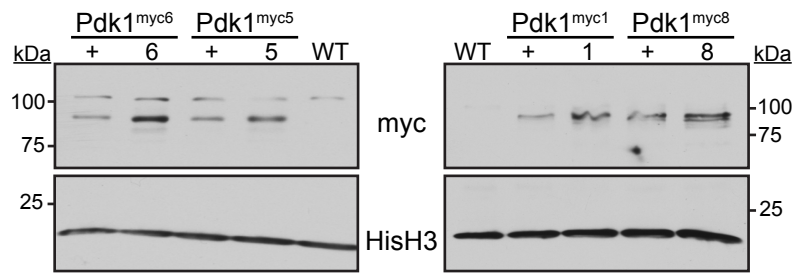

E

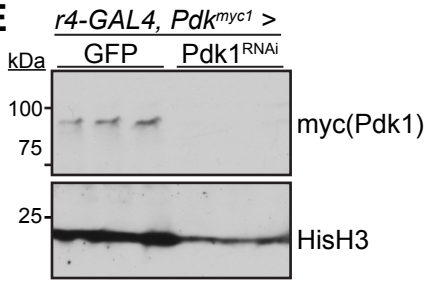

Figure S4. Design and validation of a CRISPR/Cas9 strategy to insert a myc tag at the 3' end of the *Pdk1* coding region, Related to Figure 3.

A) The final coding exons (black) and 3'UTR (gray) of *Pdk1* are depicted. The region underlined in blue corresponds to the DNA sequence in part B and is common to all *Pdk1* splice variants. Numbering above exons refers to coordinates in FlyBase release 6.10. **B)** Top: the final 272 nt encoding the carboxy-terminus of wild type *Pdk1* and the first 194 nt of the 3'UTR. Middle: the sequence of the ssDNA template for homology-directed repair following DNA cleavage by Cas9. The gRNA sequence is in bold text and underlined. Stop codons are in red, and the sequence encoding the myc tag is in blue. The 79 bp (left) and 81 bp (right) homology arms of the ssDNA oligo are highlighted in gray. Bottom: the expected DNA sequence of the targeted *Pdk1* allele. Note the mutated PAM site (italicized) present in both the ssDNA oligo and the targeted allele. Primer sequences (F1, R1, and R2) used in part C are boxed. **C)** PCR genotyping of wild type (+/+), $Pdk1^{myc}$/+, and $Pdk1^{myc}$/$Pdk1^{myc}$ flies is shown for four independent insertions: lines 5, 6, 1, and 8. Line 8 contains multiple copies of the myc insertion. **D, E)** Western blot analysis of myc (Pdk1) and HisH3 levels in **D)** adult flies that are wild type (WT), heterozygous, or homozygous for $Pdk1^{myc6}$, $Pdk1^{myc5}$, $Pdk1^{myc1}$, or $Pdk1^{myc8}$ (n = 2 flies/lane) and **E)** larval fat bodies heterozygous for $Pdk1^{myc1}$ and expressing GFP or a $Pdk1^{RNAi}$ transgene under control of the fat body driver r4-GAL4 (n = 3/gp, 10 fat bodies pooled/lane).

Figure	Genotype
1A	*w; UAS-GFP / +; r4-GAL4 / +* and *w; UAS-Toll^{10b} / +; r4-GAL4 / +*
1B	*w;* [*UAS-GFP* or *UAS-Toll^{10b}*] */ +; r4-GAL4, dilp2^{1}, gd2HF / dilp2^{1}, gd2HF*
1C	*w; UAS-GFP/+; r4-GAL4 / +* and *w; +/+; r4-GAL4/UAS-Dilp2* and *w; UAS-Toll^{10b}/+; r4-GAL4/UAS-Dilp2*
1E, left	*y, w, hsFLP / w; +/+; Act5c>Cd2>GAL4 / +*
1E, right	*y, w, hsFLP / w; +/+; Act5c>Cd2>GAL4 / UAS-Toll^{10b}*
1G, left	*y, w, hsFLP / w; UAS-InR^{A1325D} / +; Act5c>Cd2>GAL4 / +*
1G, right	*y, w, hsFLP / w; UAS-InR^{A1325D}, UAS-Toll^{10b} / +; Act5c>Cd2>GAL4 / +*
1I, left	*y, w, hsFLP / w; +/+; Act5c>Cd2>GAL4 / UAS-myrAkt*
1I, right	*y, w, hsFLP / w; UAS-Toll^{10b} / +; Act5c>Cd2>GAL4 / UAS-myrAkt*
2A-C, left	*y, w, hsFLP, UAS-Dp110^{CAAX} / w; + / +; Act5c>Cd2>GAL4 / +*
2A-C, right	*y, w, hsFLP, UAS-Dp110^{CAAX} / w; + / +; Act5c>Cd2>GAL4 / UAS-Toll^{10b}*
2D-G,	*rictor$^{\Delta 2}$ / +; +/+; r4-GAL4 / UAS-GFP*
left to right	*rictor$^{\Delta 2}$ / +; +/+; r4-GAL4 / UAS-Toll^{10b}*
	rictor$^{\Delta 2}$ / Y; +/+; r4-GAL4 / UAS-GFP
	rictor$^{\Delta 2}$ / Y; +/+; r4-GAL4 / UAS-Toll^{10b}
3A and B,	*w; UAS-GFP / +; r4-GAL4, Pdk1$^{\Delta 33}$/ TM3, Ser, GFP*
left to right	*w; UAS-Toll^{10b} / +; r4-GAL4, Pdk1$^{\Delta 33}$/ TM3, Ser, GFP*
	w; UAS-GFP / +; r4-GAL4, Pdk1$^{\Delta 33}$/ Pdk1$^{\Delta 33}$
	w; UAS-Toll^{10b} / +; r4-GAL4, Pdk1$^{\Delta 33}$/ Pdk1$^{\Delta 33}$
3C, left	*w; UAS-GFP / +; r4-GAL4 / Pdk1^{myc}*
3C, right	*w; UAS-Toll^{10b} / +; r4-GAL4 / Pdk1^{myc}*
3D, left	*y, w, hsFLP / w; + / +; Act5c>Cd2>GAL4 / UAS-Pdk1*
3D, right	*y, w, hsFLP / w; UAS- Toll^{10b} / +; Act5c>Cd2>GAL4 / UAS-Pdk1*
3F-H,	*w; UAS-RFP / +; r4-GAL4 / UAS-GFP*
left to right	*w; UAS-Toll^{10b} / +; r4-GAL4 / UAS-GFP*
	w; UAS-RFP / +; r4-GAL4 / UAS-Pdk1
	w; UAS-Toll^{10b} / +; r4-GAL4 / UAS-Pdk1
4A, left	*y, w, hsFLP / w; +/+; Act5c>Cd2>GAL4 / UAS-Akt^{T342D}*
4A, right	*y, w, hsFLP / w; UAS-Toll^{10b} / +; Act5c>Cd2>GAL4 / UAS-Akt^{T342D}*
4C & E, F	*w; UAS-RFP / +; r4-GAL4 / UAS-GFP*
left to right	*w; UAS-Toll^{10b} / +; r4-GAL4 / UAS-GFP*
	w; UAS-RFP / +; r4-GAL4 / UAS-Akt^{T342D}
	w; UAS-Toll^{10b} / +; r4-GAL4 / UAS-Akt^{T342D}
4D	*w; UAS-RFP / +; r4-GAL4 / UAS-GFP*
left to right	*w; UAS-Toll^{10b} / +; r4-GAL4 / UAS-GFP*
	w; UAS-RFP / +; r4-GAL4 / UAS-wild type Akt
	w; UAS-Toll^{10b} / +; r4-GAL4 / UAS-wild type Akt
4G	*w; + / +; r4-GAL4, UAS-Toll^{10b}/ UAS-X (X = various transgenes, as indicated)*

Table S1. Full genotypes of flies for each data point. Related to Experimental Procedures and Figures 1-4.

SUPPLEMENTAL EXPERIMENTAL PROCEDURES

Drosophila stocks used in this study

The following stocks obtained from the Bloomington *Drosophila* Stock Center (Bloomington, IN, NIH P40OD018537) were used in this study: UAS-InR^{A1325D} (#8263), UAS-Dp110^{CAAX} (#25908), UAS-RFP (#30556), UAS-GFP (2nd (#1521) and 3rd (#1522) chromosome insertions), UAS-Dif^{RNAi} (#30513), UAS-Pdk1^{RNAi} (#27725), hsFLP22 (#8862), Act5c>Cd2>Gal4 (#4780), tGPH (#8163), r4-GAL4 (#33832). Other flies used were: UAS-Toll^{10b} (Hu et al., 2004), *rictor*$^{\Delta 2}$ (Hietakangas and Cohen, 2007), UAS-Akt1.HA (wild type) and UAS-myrAkt (Verdu et al., 1999), and *Pdk1*$^{\Delta 33}$ (Cheng et al., 2011).

Construction of UAS-Akt^{T342D} and UAS-Pdk1 transgenic flies

For UAS-Akt^{T342D} and UAS-Pdk1 transgenes, full-length cDNAs (Akt: clone SD10374 and Pdk1: clone LD22131 (836 aa isoform), *Drosophila* Genomics Resource Center, Bloomington, IN, NIH 2P40OD010949) were amplified with gene-specific primers engineered to contain carboxy-terminal HA (Akt) or myc (Pdk1) tags. PCR products were cloned into pENTR (Invitrogen), and phosphorylation site mutations (including phospho-mimicking T342D) were introduced by site-directed mutagenesis (Q5 kit, New England Biolabs). Primer sequences used for cloning and site-directed mutagenesis are listed at the end of this section. Gateway cloning (Invitrogen) was used to generate pUAST-Akt^{T342D}.HA and pUAST-Pdk1.myc. Transgene constructs were injected into *Drosophila* embryos at Rainbow Transgenics (Camarillo, CA). Standard genetics was used to map and generate balanced transgenic lines.

Construction of a myc-tagged *Pdk1* allele

CRISPR/Cas9 was used to insert a myc epitope tag at the 3' end of the final coding exon of *Pdk1*, which is common to all splice variants. The Fly CRISPR Optimal Target Finder (Gratz et al., 2014) was used to identify a CRISPR target site located just upstream of the *Pdk1* stop codon (Figure S4A,B) and with only one predicted off-target site on the X chromosome (*Pdk1* is on chromosome 3). Oligos encoding the *Pdk1* CRISPR-targeting RNA were annealed and ligated into the BbsI site of pU6-BbsI-chiRNA, and PCR was used to create the template for in vitro transcription of the gRNA using the MEGAscript T7 kit (Ambion). The donor template for homology-directed repair consisted of a 200 nucleotide ssDNA oligo with 79 and 81 nt left and right homology arms flanking the myc epitope tag coding sequence, which was engineered immediately 5' of the *Pdk1* stop codon. The PAM sequence of the gRNA binding site in the donor template was mutated, and two additional stop codons in the two alternate reading frames were added downstream of the original stop codon (Figure S4B). Oligonucleotide sequences are listed at the end of this section. See Supplementary Figure 4 for further details.

The gRNA and ssDNA donor template (synthesized as a PAGE-Purified Ultramer by Integrated DNA Technologies, Coralville, IA) were analyzed by separation on a 10% TBE-Urea gel (Bio-Rad) and found to be intact and full-length. The gRNA and ssDNA donor template were injected into *nos-Cas9*/*CyO* embryos at Rainbow Transgenics (Camarillo, CA). Standard fly genetics was used to balance putative insertion lines and to remove *nos-Cas9*. Out of 120 injected embryos, 35 F0 flies were fertile, and eight F1 lines were established for each fertile F0 line. The F1 lines were screened by Western blotting for the myc epitope tag, and four F0 lines bearing the insertion were identified. PCR-based genotyping and sequencing were carried out on each of these four lines to validate insertions (Figure S4C). Insertion lines were further tested by Western blotting to assess: 1) dose-dependent increase in myc-tag signal in *Pdk1*^{myc}/+ compared with *Pdk1*^{myc}/*Pdk1*^{myc} animals (Figure S4D) and 2) elimination of myc-tag signal in fat body lysates from larvae expressing UAS-Pdk1^{RNAi} under control of r4-GAL4 (Figure S4E). We noted no fertility, viability or growth defects in flies heterozygous or homozygous for *Pdk1*^{myc} alleles compared with wild type, suggesting that the myc insertion has negligible effect on Pdk1 function. We also noted that both fat body and whole animal-lysates show that the major Pdk1 splice variant expressed in larvae is the 755 aa (85.6 kDa) form rather than the 539 or 836 aa forms (61 or 94.1 kDa). The *Pdk1*^{myc1} allele was used for protein expression experiments in Figure 3.

Whole-mount Immunocytochemistry

Fat bodies bearing clones of cells expressing UAS-transgenes, generated using the FLP; Act5c>Cd2>GAL4 system (Pignoni and Zipursky, 1997), were dissected from mid-third instar larvae. Fat bodies were fixed in 4% paraformaldehyde for 20 min, blocked in 10% normal donkey and goat sera (Jackson ImmunoResearch) in PBS with 0.1% Triton X-100 (10% ND/GS-T) for 30 min, then incubated overnight at 4°C with mouse anti-Cd2 and rabbit anti-GFP (to detect tGPH) or rabbit anti-phosphoSer505-Akt, diluted in 1% ND/GS-T. The next day, fat bodies were washed in 1% ND/GS-T, incubated with goat anti-rabbit Alexa488 and donkey anti-mouse Cy3 secondary antibodies, diluted in 1% ND/GS-T, for 2 h at room temperature, counterstained with DAPI (Sigma-Aldrich), and mounted on slides in Fluoromount G (Electron Microscopy Sciences).

Western blot analysis

Whole larvae or adult flies (2/sample) or dissected fat bodies (6-10 pooled/sample) were sonicated in 2% SDS and 60 mM Tris-HCl, pH 6.8 with protease inhibitors (Roche Diagnostics) and phosphatase inhibitors. Equal amounts of protein (10-30 µg, measured by BCA assay, Pierce) were separated by SDS-PAGE, proteins were transferred to nitrocellulose, blocked in 3% milk in TBS with 0.1% Tween-20 (TBS-T), and blotted overnight at 4˚C with primary antibodies diluted in 1% milk in TBS-T. Following washes, blots were incubated with secondary antibodies in 1% milk in TBS-T, washed again, incubated with ECL (Pierce), and exposed to film. For phospho-specific antibodies, nitrocellulose membranes were blocked in 3% BSA in TBS-T, and blotted overnight at 4˚C with primary antibodies diluted in 1% BSA in TBS-T. Wash steps, secondary antibody incubation, and detection were performed as described above.

Antibodies used in this study, dilutions, catalog numbers and sources

Immunocytochemistry:
rat anti-mouse Cd2, 1:8000 (MCA154GA, AbD Serotec)
rabbit anti-GFP, 1:8000 (A11122, Invitrogen)
donkey anti-mouse Cy3, 1:300 (715-165-150, Jackson ImmunoResearch)
goat anti-rabbit Alexa488, 1:300 (111-545-003, Jackson ImmunoResearch)

Western blotting:
rabbit anti-phosphoSer505-Akt, 1:1000 (same dilution for immunocytochemistry, 4054, Cell Signaling Technology)
rabbit anti-mouse Akt, 1:1000 (9272, Cell Signaling Technology)
mouse anti-myc tag, 1:5000 (2276, Cell Signaling Technology)
rabbit anti-human Histone H3, 1:5000 (4499, Cell Signaling Technology)
goat anti-rabbit HRP, 1:10,000 (111-035-003, Jackson ImmunoResearch)
goat anti-mouse HRP, 1:10,000 (115-035-003, Jackson ImmunoResearch)

Quantitative RT-PCR

Total RNA was isolated from mid-third instar larval fat bodies (n = 6-8 pooled/sample) using the Reliaprep Tissue RNA Miniprep kit (Promega). Reverse transcription was performed on 1-2 µg total RNA using the ProtoScript First Strand cDNA Synthesis kit (New England Biolabs). Quantitative PCR reactions were performed on 20 ng cDNA, in triplicate, on a Bio-Rad CFX Connect Real-Time PCR Detection System using SYBR Select Master Mix (Life Technologies). Relative amounts of transcripts were calculated using the comparative C_T method using *Rp49* as a reference gene (Schmittgen and Livak, 2008). Gene-specific primer sequences are listed on the next page.

Primers and oligonucleotides used in this study (all listed 5' to 3')

Cloning primers, UAS-Akt-HA and UAS-Pdk1-myc:

Akt-F	CACCATGTCAATAAACACAACTTTCGACC
Akt-HA-R	CTAGGCGTAATCGGGCACATCGTAGGGGTACATTTGCATCGATGCGAGACTTGTGG
Pdk1-F	CACCATGCCGGCTATGGCCAAGGAGAAAGCATCAGC
Pdk1-myc-R	TTACAGATCCTCCTCGGAGATCAGCTTCTGCTCCATCTTAGACGCCGTCTTCTTGCTAGGTGACG

Site-directed mutagenesis primers to generate Akt point mutants:

T342D-F	AGACTTCTGCGGTACACCGGAATAC
T342D-R	TTAGTTGTGCGGCCGTAGGTGAT
T342A-F	AGCTTTCTGCGGTACACCGGAATAC
T342A-R	TTAGTTGTGCGGCCGTAGGTGAT
S505A-F	TTCGCCTACCAAGGAGACATGGCC
S505A-R	CTGGGGGAAAAGCGGCTCTTCGGC
S505D-F	CCAGGGAGACATGGCCTCCACG
S505D-R	TAGTCGAACTGCGGGAAAAGCGG

Primers for synthesis of *Pdk1* gRNA:

Pdk1-myc-gRNA-F	CACCGACGTCACCTAGCAAGAAGA
Pdk1-myc-gRNA-R	AAACTCTTCTTGCTAGGTGACGTC
T7-sgR-F	TTAATACGACTCACTATAGGACGTCACCTAGCAAGAAGAGTTTTAGAGCTAGAAATAG
T7-sgR-R	AAAAGCACCGACTCGGTGCC

ssDNA homology-directed repair template:

AGCTTCGACGGCGTCTGACAACCGGACATTGGGTAGCACCAGAACGGGGACGTCACCTAGCAAGAAGACAACGTCTAAGA
TGGAGCAGAAGCTGATCTCCGAGGAGGATCTGTAAATAACGTAGTCCTATTTATAGCAATGTGAAATTAATTTAGTTGAA
ATTTAGTGCAAACGAAGCGATGGCGTAGAAGAGGGCGGGA

Genotyping: *Pdk1^{myc}* allele generated with CRISPR/Cas9:

Pdk1-myc-F1	ATGCTATCCACTGGTCGGAAG
Pdk1-myc-R1	CCTAAGCACAATACAAATCGGA
Pdk1-myc-R2	CTCGGAGATCAGCTTCT

Primers for Q-PCR:

InR-F	GCCAATTCAATAGCGGGATAC
InR-R	CTCGCATAGAACGGATTCACC
chico-F	CGTCGGAAAAGCTTGCTAAG
chico-R	GTCCCGTATCATTCAAGTGTC
PI3K92E-F	TACTGGACTACGCCTATCCAG
PI3K92E-R	CTTTCCAGGTACGATTCGTGC
Pten-F	GCCACAGAAAATGCAAAGCCA
Pten-R	GCCGGAAACTGGTATTGATGGT
Pdk1-F	CGCGACTCATCTATATCGATC
Pdk1-R	GTCAGACGCCGTCGAAGCTTG
Akt-F	ATGACGCCATCTGAACAGAC
Akt-R	CTTCTCGCGACACAAAATAACC
rictor-F	CCGTAAAAGGCATCGAAGTAC
rictor-R	GTGGTAGCTTCTCGTAGCTGTA
Tor-F	ATTTGGGTGAGGGAGAGCATC
Tor-R	CTGCTCCAAAACATTGTCGC
Phlpp-F	ACTTGCAGTTGCAGGTGGAC
Phlpp-R	ATCGACTAGGCTCCAATGGC
Drs-F	ACCAAGCTCCGTGAGAACCT
Drs-R	CTTGCACACACGACGACAG
Rp49-F	GACGCTTCAAGGGACAGTATCTG
Rp49-R	AAACGCGGTTCTGCATGA

SUPPLEMENTAL REFERENCES

Andjelkovic, M., Jones, P.F., Grossniklaus, U., Cron, P., Schier, A.F., Dick, M., Bilbe, G., and Hemmings, B.A. (1995). Developmental regulation of expression and activity of multiple forms of the Drosophila RAC protein kinase. J. Biol. Chem. *270*, 4066–4075.

Cheng, L., Locke, C., and Davis, G.W. (2011). S6 kinase localizes to the presynaptic active zone and functions with PDK1 to control synapse development. J. Cell Biol. *194*, 921–935.

Gratz, S.J., Ukken, F.P., Rubinstein, C.D., Thiede, G., Donohue, L.K., Cummings, A.M., and O'Connor-Giles, K.M. (2014). Highly Specific and Efficient CRISPR/Cas9-Catalyzed Homology-Directed Repair in Drosophila. Genetics *196*, 961–971.

Hietakangas, V., and Cohen, S.M. (2007). Re-evaluating AKT regulation: role of TOR complex 2 in tissue growth. Genes Dev. *21*, 632–637.

Hu, X., Yagi, Y., Tanji, T., Zhou, S., and Ip, Y.T. (2004). Multimerization and interaction of Toll and Spätzle in Drosophila. Proc. Natl. Acad. Sci. U.S.a. *101*, 9369–9374.

Pignoni, F., and Zipursky, S.L. (1997). Induction of Drosophila eye development by decapentaplegic. Development *124*, 271–278.

Schmittgen, T.D., and Livak, K.J. (2008). Analyzing real-time PCR data by the comparative C(T) method. Nat Protoc *3*, 1101–1108.

Verdu, J., Buratovich, M.A., Wilder, E.L., and Birnbaum, M.J. (1999). Cell-autonomous regulation of cell and organ growth in Drosophila by Akt/PKB. Nat. Cell Biol. *1*, 500–506.